# On the Spectrum of Multi-Space Euclidean Random Matrices

Aldo Battista, Remi Monasson

# On the Spectrum of Multi-Space Euclidean Random Matrices

Aldo Battista and Rémi Monasson*
*Laboratory of Physics of the Ecole Normale Supérieure, CNRS UMR 8023 & PSL Research, Sorbonne Université, 24 rue Lhomond, 75005 Paris, France*
(Dated: March 16, 2020)

We consider the additive superimposition of an extensive number of independent Euclidean Random Matrices in the high-density regime. The resolvent is computed with techniques from free probability theory, as well as with the replica method of statistical physics of disordered systems. Results for the spectrum and eigenmodes are shown for a few applications relevant to computational neuroscience, and are corroborated by numerical simulations.

## I. INTRODUCTION

In the twenty years following their introduction, Euclidean Random Matrices (ERM) have been studied in a variety of contexts in physics and mathematics [1]. Examples of applications of ERM include the theoretical description of vibrations in topologically disordered systems [2–4], wave propagation in random media [5, 6], relaxation in glasses [7], Anderson localization [8] and many more [9].

While determining the spectral properties of ERM is generally quite involved due to the existence of correlations between the entries of these matrices, a well-understood limit is the so-called high-density regime [1, 10]. Assume $N$ points $\mathbf{r}_i$ are drawn uniformly at random in a bounded space, *i.e.*, the unit $D$-dimensional hypercube $\mathcal{H}_D$, and define the $N$-dimensional ERM $\mathbf{C}$ with entries $C_{ij} = \Gamma(|\mathbf{r}_i - \mathbf{r}_j|)/N$. Here, $|\cdot|$ denotes the Euclidean distance (with periodic boundary conditions over $\mathcal{H}_D$), and $\Gamma$ is a given function. In the large-$N$ limit (for fixed $D$), the points effectively form a dense, statistically uniform sampling of the hypercube; the eigenmodes of $\mathbf{C}$ are well approximated by Fourier plane waves, with eigenvalues

$$\hat{\Gamma}(\mathbf{k}) = \int_{\mathcal{H}_D} d\mathbf{r}\, e^{i\,2\pi\,\mathbf{k}\cdot\mathbf{r}}\,\Gamma(\mathbf{r}) \ , \tag{1}$$

where the components of $\mathbf{k} = (k_1, k_2, ..., k_D)$ are integer-valued.

Hereafter, we introduce a novel statistical ensemble of ERMs in the high-density regime obtained by mixing multiple spaces. Instead of having a single set of $N$ random points $\mathbf{r}_i$, we consider $L$ such sets, $\mathbf{r}_i^\ell$, with $\ell = 1, ..., L$ (and $i = 1, ..., N$ as usual). Each index $\ell$ point to a different "space" (hypercube), and for simplicity all points are drawn uniformly at random in the different spaces. We define the superimposition of all the ERM attached to the spaces, with entries

$$C_{ij} = \frac{1}{L}\sum_{\ell=1}^{L} \Gamma\left(\left|\mathbf{r}_i^\ell - \mathbf{r}_j^\ell\right|\right) \ . \tag{2}$$

We refer to such matrices as Multispace-ERM (MERM). To our knowledge, MERM have not been considered so far in statistical physics. Our motivation to study MERM arises from computational neuroscience, more precisely, the need to understand how the hippocampal network can account for multiple cognitive maps, coding for various environmental and contextual situations [11]. The resulting statistical ensemble for MERM is sketched in Fig. 1.

A non trivial statistical setting is obtained when the number $L$ of spaces is of the order of the matrix size, $N$. More precisely, we consider herefater the double infinite limit $L, N \to \infty$ at fixed ratio

$$\alpha = \frac{L}{N} \ . \tag{3}$$

Our paper is organized as follows. The spectrum of MERM is computed using free probability theory in Section 2, and re-derived using the replica method in Section 3. We show the results for the spectrum and eigenmodes for the choice of $\Gamma$ corresponding to Fig. 1 and compare with numerical simulations in Section 4. Variations on the choice of $\Gamma$ are discussed in Section 5. Last of all, Section 6 presents some conclusions.

*Electronic address: monasson@lpt.ens.fr

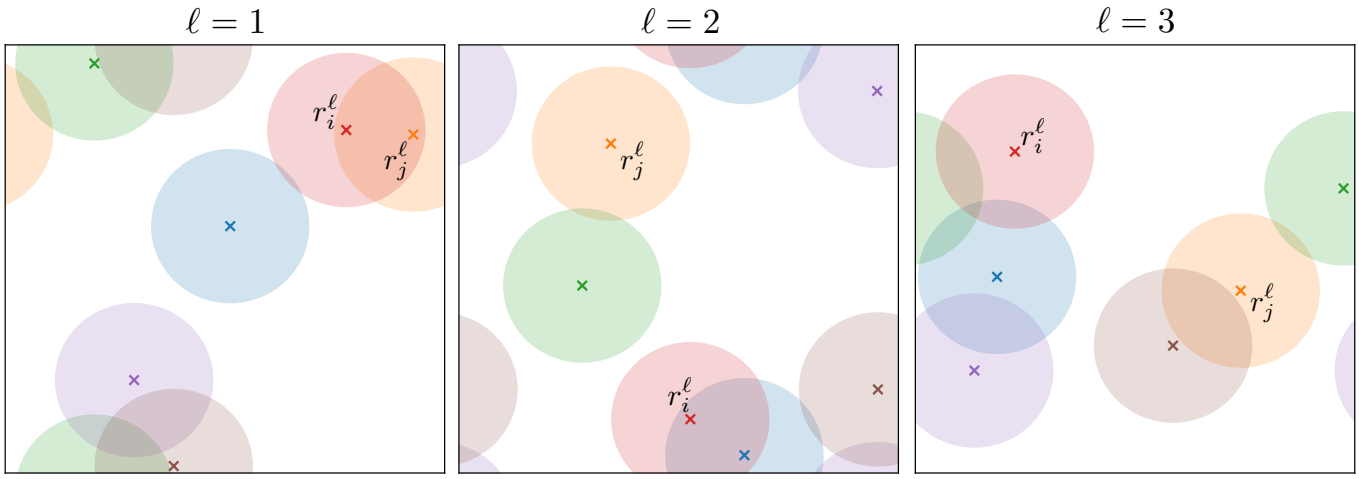


FIG. 1: Basic statistical ensemble of MERM considered in this work. $L = 3$ sets of $N = 5$ points, $\mathbf{r}_i^\ell$, with $\ell = 1, ..., L$ and $i = 1, ..., N$ are drawn uniformly at random in unit squares $\mathcal{H}_2$ (dimension $D = 2$). Points are represented by crosses, whose colors identify their indices $i$. The MERM is defined through (2), where $\Gamma$ is a generic function of the distance between points. A possible choice for $\Gamma$, inspired from the so-called place cells in neuroscience, is the overlap (common area) between pairs of disks of surface $\phi_0 < 1$ and having centers $\mathbf{r}_i^\ell$ in each space $\ell$.

## II. SPECTRUM OF MERM: FREE-PROBABILITY-BASED DERIVATION

### A. Case of a single space ($L = 1$)

We consider the ERM defined from $N$ points $\mathbf{r}_i$ drawn uniformly at random in the $D$-dimensional unit hypercube $\mathcal{H}_D$:

$$M_{ij}^{(1)} = \frac{1}{N}\,\Gamma(|\mathbf{r}_i - \mathbf{r}_j|)\ . \tag{4}$$

In the $N \to \infty$ limit, the eigenvalues of $\mathbf{M}^{(1)}$ are the Fourier coefficients (1) of $\Gamma$, where $\mathbf{k} \in \mathbb{Z}^D$ and with associated eigenvectors of components $v_i(\mathbf{k}) \simeq e^{i\,2\pi\,\mathbf{k}\cdot\mathbf{r}_i}/\sqrt{N}$ [1, 10]. The resolvent (Stieltjes transform) of $\mathbf{M}^{(1)}$ is defined as

$$s_1(z) = \frac{1}{N}\Big\langle \text{Trace}\,\left(\mathbf{M}^{(1)} - z\,\mathbf{Id}\right)^{-1}\Big\rangle_{(1)}\ , \tag{5}$$

where $\langle\cdot\rangle_{(1)}$ stands for the average over the distribution of the matrix (4). It is then easy to rewrite the resolvent when $N \gg 1$,

$$s_1(z) = -\frac{1}{zN}\Big(N + \sum_{\ell=1}^{\infty}\sum_{\mathbf{k}}^{(N)}\hat{\Gamma}(\mathbf{k})^\ell\,\frac{1}{z^\ell}\Big) = -\frac{1}{z} - \frac{1}{N\,z}\,\gamma\left(\frac{1}{z}\right) + o\left(\frac{1}{N}\right) \tag{6}$$

with

$$\gamma(u) = \sum_{\mathbf{k}}\frac{u\,\hat{\Gamma}(\mathbf{k})}{1 - u\,\hat{\Gamma}(\mathbf{k})} \tag{7}$$

and where the sum runs over $\mathbb{Z}^D$.

### B. Case of multiple spaces ($L = \alpha N$)

We consider now the case of an extensive number $L$ of spaces, see (3), with

$$M_{ij}^{(L)} = \frac{1}{N}\sum_{\ell=1}^{L}\Gamma\left(|\mathbf{r}_i^\ell - \mathbf{r}_j^\ell|\right)\ , \tag{8}$$

where the points are independently drawn from one space $\ell$ to another. According to free-probability theory [12, 13], the resolvent $s_L(z)$ of $\mathbf{M}^{(L)}$ can be computed through the following steps:

1. Invert (functionally) the resolvent $s_1(z)$ of $\mathbf{M}^{(1)}$: using (6) we obtain

$$z_1(s) = -\frac{1}{s} - \frac{\gamma(-s)}{N\,s} + o\left(\frac{1}{N}\right) \ . \tag{9}$$

2. Compute the $R$-transform of $\mathbf{M}^{(1)}$, defined through

$$R_1(s) \equiv z_1(-s) - \frac{1}{s} \ . \tag{10}$$

   Using (9), we obtain

$$R_1(s) = \frac{\gamma(s)}{N\,s} + o\left(\frac{1}{N}\right) \ . \tag{11}$$

3. Compute the $R$-transform of $\mathbf{M}^{(L)}$ through

$$R_L(s) = L\ R_1(s) \ . \tag{12}$$

   Using (11), we obtain,

$$R_L(s) = \alpha\frac{\gamma(s)}{s} + o(1) \ , \tag{13}$$

   where the corrections $o(1)$ vanish when both $N, L \to \infty$ at fixed ratio $\alpha$.

4. Write the functional inverse resolvent of $\mathbf{M}^{(L)}$ through

$$z_L(s) = R_L(-s) - \frac{1}{s} = -\frac{1+\alpha\,\gamma(-s)}{s} \ . \tag{14}$$

5. Compute the resolvent $s_L(z)$ of $\mathbf{M}^{(L)}$. From (14) and (7) we find the implicit equation satisfied by $s_L$:

$$z = \alpha \sum_{\mathbf{k}} \frac{\hat{\Gamma}(\mathbf{k})}{1 + s_L\,\hat{\Gamma}(\mathbf{k})} - \frac{1}{s_L} \ . \tag{15}$$

Note that we are eventually interested in the spectral properties of the matrix $\mathbf{C}$ with entries

$$C_{ij} = \frac{1}{L}\sum_{\ell=1}^{L} \Gamma\left(\left|\mathbf{r}_i^\ell - \mathbf{r}_j^\ell\right|\right) = \frac{1}{\alpha} M_{ij}^{(L)} \ . \tag{16}$$

Obviously, the resolvent $s$ of $\mathbf{C}$ is related to the resolvent $s_L$ of $\mathbf{M}^{(L)}$ through the equation $s(z) = \alpha\, s_L(\alpha\, z)$. Hence we obtain our fundamental implicit equation for the resolvent of $\mathbf{C}$:

$$z = \sum_{\mathbf{k}} \frac{\alpha\,\hat{\Gamma}(\mathbf{k})}{\alpha + s\,\hat{\Gamma}(\mathbf{k})} - \frac{1}{s} \ . \tag{17}$$

A caveat about the use of free probability theory is needed here. Informally speaking, free probability theory applies if the eigenbasis of the correlation matrices $\mathbf{M}^{(1)}$ attached to the different spaces $\ell$ are orthogonal with high probability. This assumption holds here only in the subspace orthogonal to the $\mathbf{k} = \mathbf{0}$ eigenmode common to all subspaces. Hence, this eigenmode (whose all components are asymptotically equal to $N^{-1/2}$) corresponds to an extensive eigenvalue of $\mathbf{C}$ equal to

$$z_{ext} \simeq N\,\hat{\Gamma}(\mathbf{0}) \ , \tag{18}$$

which is not captured by the resolvent $s(z)$. Accordingly, the sum over $\mathbf{k}$ in (15) and (17) runs overs all non-zero vectors in $\mathbb{Z}^D$.

## III. SPECTRUM OF MERM: REPLICA-BASED DERIVATION

Here we re-derive the implicit equation (15) for the resolvent of $\mathbf{M}^{(L)}$ using the replica method coming from statistical physics of disordered systems. We start by rewriting the definition of the resolvent as

$$s_L(z) = \frac{1}{N}\Big\langle \text{Trace } \big(\mathbf{M}^{(L)} - z\,\mathbf{Id}\big)^{-1}\Big\rangle = \frac{2}{N}\partial_z\Big\langle \log\det\big(\mathbf{M}^{(L)} - z\,\mathbf{Id}\big)^{-\frac{1}{2}}\Big\rangle\ , \tag{19}$$

where $\langle\cdot\rangle$ stands for the average over the distribution of the matrix (8). With this representation the determinant $\det\big(\mathbf{M}^{(L)} - z\,\mathbf{Id}\big)^{-\frac{1}{2}}$ can be expressed as a canonical partition function:

$$\mathcal{Z}_L(s) = \det\big(\mathbf{M}^{(L)} - z\,\mathbf{Id}\big)^{-\frac{1}{2}} = \int\prod_i \frac{d\phi_i}{\sqrt{2\pi}}\exp\Big(\frac{z}{2}\sum_i\phi_i^2 - \frac{1}{2}\sum_{ij}\phi_i M^{(L)}_{ij}\phi_j\Big)\ , \tag{20}$$

where $i, j$ go from 1 to $N$. The resolvent (19) can be calculated using the replica trick [14]:

$$s_L(z) = \frac{2}{N}\partial_z\big\langle\log\mathcal{Z}_L(s)\big\rangle = \frac{2}{N}\partial_z\Big[\lim_{n\to 0}\frac{1}{n}\log\big\langle\mathcal{Z}_L(s)^n\big\rangle\Big] \tag{21}$$

with

$$\big\langle\mathcal{Z}_L(s)^n\big\rangle = \int\prod_{ia}\frac{d\phi_i^a}{\sqrt{2\pi}}\exp\Big(\frac{z}{2}\sum_a\sum_i(\phi_i^a)^2\Big)\Big\langle\exp\Big(-\frac{1}{2}\sum_a\sum_{ij}\phi_i^a M^{(L)}_{ij}\phi_j^a\Big)\Big\rangle\ , \tag{22}$$

where we have replicated the system $n$ times, *i.e.*, $a$ goes from 1 to $n$.

In order to perform the average in (22) we rewrite (8) by considering the $\ell$-th space ERM in its eigenbasis:

$$M^{(L)}_{ij} = \frac{1}{N}\sum_{\ell=1}^{L}\Gamma\big(|\mathbf{r}_i^\ell - \mathbf{r}_j^\ell|\big) = \sum_\ell\sum_{\mathbf{k}\neq\mathbf{0}} v^\ell_{\mathbf{k}i}\ \hat\Gamma(\mathbf{k})\ v^\ell_{\mathbf{k}j}\ , \tag{23}$$

where $\ell$ goes from 1 to $L$, and the sum over $\mathbf{k}$ discards the $\mathbf{k}=\mathbf{0}$ extensive mode as discussed in the section above. The eigenvector components, $v^\ell_{\mathbf{k}i}\simeq\frac{1}{\sqrt{N}}\sin\big(2\pi\,\mathbf{k}\cdot\mathbf{r}_i^\ell\big)$, $\frac{1}{\sqrt{N}}\cos\big(2\pi\,\mathbf{k}\cdot\mathbf{r}_i^\ell\big)$, are real due to the symmetry $\hat\Gamma(\mathbf{k}) = \hat\Gamma(-\mathbf{k})$. Hence we get

$$\Big\langle\exp\Big(-\frac{1}{2}\sum_a\sum_{ij}\phi_i^a M^{(L)}_{ij}\phi_j^a\Big)\Big\rangle = \Big\langle\exp\Big(-\frac{1}{2}\sum_{a,\ell,\mathbf{k}\neq\mathbf{0}}\hat\Gamma(\mathbf{k})\big(\sum_i v^\ell_{\mathbf{k}i}\phi_i^a\big)^2\Big)\Big\rangle\ . \tag{24}$$

We now use the Stratonovich trick to linearize $\big(\sum_i v^\ell_{\mathbf{k}i}\phi_i^a\big)^2$:

$$\begin{aligned}&\Big\langle\exp\Big(-\tfrac{1}{2}\textstyle\sum_{a,\ell,\mathbf{k}\neq\mathbf{0}}\hat\Gamma(\mathbf{k})\big(\sum_i v^\ell_{\mathbf{k}i}\phi_i^a\big)^2\Big)\Big\rangle \\ &= \textstyle\prod_\ell\int\prod_{a,\mathbf{k}\neq\mathbf{0}}\frac{du^a_{\ell,\mathbf{k}}}{\sqrt{2\pi}}\exp\Big(-\frac{1}{2}\sum_{a,\mathbf{k}\neq\mathbf{0}}\big(u^a_{\ell,\mathbf{k}}\big)^2\Big)\Big\langle\exp\Big(-i\sum_{a,\mathbf{k}\neq\mathbf{0}}\sqrt{\hat\Gamma(\mathbf{k})}\,u^a_{\ell\mathbf{k}}\sum_i\phi_i^a v^\ell_{\mathbf{k}i}\Big)\Big\rangle\ .\end{aligned} \tag{25}$$

Using the fact that $\langle v^\ell_{\mathbf{k}i}\rangle = 0$ and $\langle v^\ell_{\mathbf{k}i}v^{\ell'}_{\mathbf{k}'j}\rangle = \frac{1}{N}\,\delta_{ij}\delta_{\mathbf{k}\mathbf{k}'}$ it is easy to perform the average in the above equation, with the result

$$\Big\langle\exp\Big(-i\sum_{a,\mathbf{k}\neq\mathbf{0}}\sqrt{\hat\Gamma(\mathbf{k})}\,u^a_{\ell\mathbf{k}}\sum_i\phi_i^a v^\ell_{\mathbf{k}i}\Big)\Big\rangle = \exp\Big(-\frac{1}{2}\sum_{a,b}\sum_{\mathbf{k}\neq\mathbf{0}}\hat\Gamma(\mathbf{k})q^{ab}u^a_{\ell\mathbf{k}}u^b_{\ell\mathbf{k}}\Big) \tag{26}$$

where we have defined the overlap $q^{ab}$ as

$$q^{ab} = \frac{1}{N}\sum_i\phi_i^a\phi_i^b \tag{27}$$

to be fixed through

$$1 = \int\prod_{a\le b}\frac{d\hat q^{ab}dq^{ab}}{\frac{2\pi i}{N}}\exp\Big(N\sum_{a\le b}\hat q^{ab}q^{ab} - \sum_{a\le b}\hat q^{ab}\sum_i\phi_i^a\phi_i^b\Big)\ . \tag{28}$$

We can finally write $\langle \mathcal{Z}_L(s)^n \rangle$ as

$$\langle \mathcal{Z}_L(s)^n \rangle = \int \prod_{a\leq b} \frac{d\hat{q}^{ab} dq^{ab}}{\frac{2\pi i}{N}} \exp\left\{ N \left[ \log \int \prod_a \frac{d\phi^a}{\sqrt{2\pi}} \exp\Big( \frac{z}{2} \sum_a (\phi^a)^2 - \sum_{a\leq b} \hat{q}^{ab} \phi^a \phi^b \Big) \right.\right. \\ \left.\left. + \sum_{a\leq b} \hat{q}^{ab} q^{ab} + \alpha \log \int \prod_{\mathbf{k}\neq \mathbf{0},a} \frac{du^a_{\mathbf{k}}}{\sqrt{2\pi}} \exp\Big( -\frac{1}{2} \sum_{\mathbf{k}\neq\mathbf{0},a} (u^a_{\mathbf{k}})^2 - \frac{1}{2} \sum_{\mathbf{k}\neq\mathbf{0}} \sum_{a\leq b} \hat{\Gamma}(\mathbf{k}) q^{ab} u^a_{\mathbf{k}} u^b_{\mathbf{k}} \Big) \right] \right\} . \tag{29}$$

The Gaussian integrals over $\phi^a$ and $u^a_{\mathbf{k}}$ can be easily computed. We then make the Replica Symmetric (RS) Ansatz on the structure of the order parameters $q^{ab}$ and their conjugate variables $\hat{q}^{ab}$, so that

$$q^{ab} = r + (q-r)\delta_{ab} \tag{30}$$

and

$$\hat{q}^{ab} = \hat{r} + (\hat{q} - \hat{r})\delta_{ab} \ . \tag{31}$$

The integrals over $q$, $r$, $\hat{q}$ and $\hat{r}$ are then estimated using the saddle-point method valid for large $N$, and then taking the small $n$ limit. The resulting expression for the resolvent of (8) is

$$s_L(z) = 2\partial_z \Big[ \mathrm{opt}_{q,r,\hat{q},\hat{r}} \lim_{n\to 0} \lim_{N\to\infty} \frac{1}{nN} \log \langle \mathcal{Z}_L(s)^n \rangle \Big] = 2\partial_z \Big[ \mathrm{opt}_{q,r,\hat{q},\hat{r}} f(q,r,\hat{q},\hat{r}) \Big] \ , \tag{32}$$

where $f$ is the free energy density equal to

$$f(q,r,\hat{q},\hat{r}) = \hat{q}q - \frac{1}{2}\hat{r}r - \frac{\alpha}{2} \sum_{\mathbf{k}\neq\mathbf{0}} \left[ \log\Big(1 + \hat{\Gamma}(\mathbf{k})(q-r)\Big) + \frac{\hat{\Gamma}(\mathbf{k}) r}{1 + \hat{\Gamma}(\mathbf{k})(q-r)} \right] \\ - \frac{1}{2} \log\Big(2\hat{q} - \hat{r} - z\Big) - \frac{\hat{r}}{2(2\hat{q} - \hat{r} - z)} \tag{33}$$

The saddle-point equations obtained by optimizing $f(q,r,\hat{q},\hat{r})$ with respect to $\hat{q}$, $\hat{r}$, $q$ and $r$ read

$$\begin{aligned} q &= -\frac{\hat{r}}{\big(2\hat{q} - \hat{r} - z\big)^2} + \frac{1}{2\hat{q} - \hat{r} - z} \ , \quad r = -\frac{\hat{r}}{\big(2\hat{q} - \hat{r} - z\big)^2} \ , \\ \hat{q} &= \frac{\alpha}{2} \sum_{\mathbf{k}\neq\mathbf{0}} \left( \frac{\hat{\Gamma}(\mathbf{k})}{1 + \hat{\Gamma}(\mathbf{k})(q-r)} - \frac{r\ \hat{\Gamma}(\mathbf{k})^2}{\big(1 + \hat{\Gamma}(\mathbf{k})(q-r)\big)^2} \right) , \\ \hat{r} &= -\alpha \sum_{\mathbf{k}\neq\mathbf{0}} \frac{r\ \hat{\Gamma}(\mathbf{k})^2}{\big(1 + \hat{\Gamma}(\mathbf{k})(q-r)\big)^2} \ . \end{aligned} \tag{34}$$

This system of equations admits $r = \hat{r} = 0$ as a solution, which gives, according to (32), the following implicit equation satisfied by $s_L(z)$:

$$z = \alpha \sum_{\mathbf{k}\neq\mathbf{0}} \frac{\hat{\Gamma}(\mathbf{k})}{1 + s_L\, \hat{\Gamma}(\mathbf{k})} - \frac{1}{s_L} \ . \tag{35}$$

This equation is identical to (15) obtained using free probability theory.

## IV. APPLICATION AND COMPARISON WITH NUMERICS

### A. Numerical computation of the spectrum

We now aim at solving the implicit equation (17) satisfied by the resolvent of $\mathbf{C}$. We show in Fig. 2(a) the representative curve of $z$ as a function of $s$ around the pole at the origin ($s = 0$). A set of forbidden disjoint intervals, $z \in [z_-^{(m)}, z_+^{(m)}]$, with $m = 1, ..., M$ is found, which cannot be reached for real-valued $s$; the number $M$ of these intervals

is a decreasing function of the ratio $\alpha$. When $z$ lies in one of these intervals, we look for a solution to equation (17) with

$$s = s_r + i\, s_i \ , \tag{36}$$

where the imaginary part $s_i$ is strictly positive; the density of eigenvalues in $z$ is given by $\rho(z) = s_i/\pi$ by virtue of well-known properties of the Stieljes transform.

The implicit equations fulfilled by $s_r$ and $s_i$ for $z \in [z_-^{(m)}, z_+^{(m)}]$, with $m = 1, ..., M$ read

$$z = \sum_{\mathbf{k}\neq\mathbf{0}} \frac{\alpha^2\, \hat{\Gamma}(\mathbf{k})}{\left(\alpha + s_r\, \hat{\Gamma}(\mathbf{k})\right)^2 + \left(s_i\, \hat{\Gamma}(\mathbf{k})\right)^2} \ , \tag{37}$$

$$\frac{1}{s_r^2 + s_i^2} = \sum_{\mathbf{k}\neq\mathbf{0}} \frac{\alpha\, \hat{\Gamma}(\mathbf{k})^2}{\left(\alpha + s_r\, \hat{\Gamma}(\mathbf{k})\right)^2 + \left(s_i\, \hat{\Gamma}(\mathbf{k})\right)^2} \ , \tag{38}$$

and can be solved numerically. Fig. 3 shows the density of eigenvalues for various values of $\alpha$. We observe the presence of the disconnected intervals $[z_-^{(m)}; z_+^{(m)}]$ corresponding to non-zero density $\rho(z)$, referred to as "blobs" below. These blobs originate from the discrete spectrum of ERM (with eigenvalues labelled by $\mathbf{k}$) and progressively merge as $\alpha$ increases (Fig. 2(b)). We now discuss the mechanism leading to merging in the large $|\mathbf{k}|$, small $\alpha$ regime.

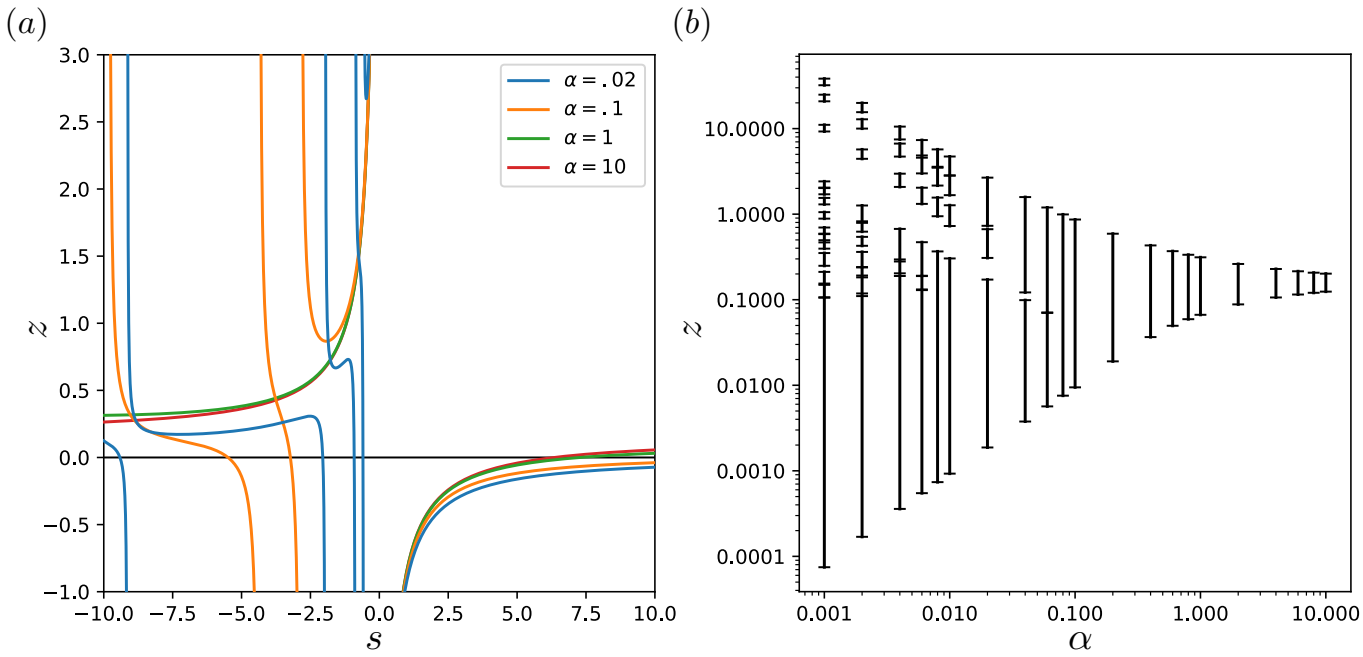


FIG. 2: ($a$) $z$ vs. $s$, see (17), close to the origin ($s = 0$), for different values of $\alpha$. ($b$) Support of the spectrum for different values of $\alpha$: black segments show the interval of eigenvalues $z$ with non-zero density $\rho(z)$. Results obtained by taking for $\Gamma$ the overlap (common length) between segments of length $\phi_0 = .2$, centered in points $\mathbf{r}_i^\ell$ randomly drawn in the unit interval $\mathcal{H}_1$ ($D = 1$).

### B. Merging of density "blobs": behavior of the density at small $\alpha$

For small $\alpha$, we look for a solution of equation (17) near the poles, so that to consider only a value $\mathbf{k} \neq \mathbf{0}$ in the sum over the modes:

$$z(\mathbf{k}) = \frac{\alpha\, \hat{\Gamma}(\mathbf{k})}{\alpha + s(\mathbf{k})\, \hat{\Gamma}(\mathbf{k})} - \frac{1}{s(\mathbf{k})} \ . \tag{39}$$

We find then $s(\mathbf{k})$ such that $\frac{dz(\mathbf{k})}{ds(\mathbf{k})} = 0$, *i.e.*, where the resolvent has singularities (eigenvalues), obtaining:

$$s_\pm(\mathbf{k}) = -\frac{\alpha}{\hat{\Gamma}(\mathbf{k})}\big(1 \pm \sqrt{\alpha}\big) \ , \tag{40}$$

this implies that the spectrum has the edges located at:

$$z_\pm(\mathbf{k}) = \frac{\hat{\Gamma}(\mathbf{k})}{\alpha}\big(1 \pm 2\sqrt{\alpha}\big) \ . \tag{41}$$

This means that when $\alpha$ become sufficiently small the spectrum develop a blob in correspondence of every $\mathbf{k} \neq \mathbf{0}$ centered in $z_\mathbf{k} = \frac{1}{2}(z_-(\mathbf{k}) + z_+(\mathbf{k})) = \frac{\hat{\Gamma}(\mathbf{k})}{\alpha}$ and of half-width $\frac{1}{2}(z_+(\mathbf{k}) - z_-(\mathbf{k})) = \frac{2\hat{\Gamma}(\mathbf{k})}{\sqrt{\alpha}}$. In order now to understand how the density of eigenvalues behaves inside this blobs we look to a solution of equation (39) of the form

$$s(\mathbf{k}) = s_r(\mathbf{k}) + i\, s_i(\mathbf{k}) \ , \tag{42}$$

so that to finally obtain the parametric equations for the density $\rho(z)$ of eigenvalues equal to $z$:

$$\rho(x;\mathbf{k}) = \frac{\alpha^{\frac{3}{2}}}{\pi\hat{\Gamma}(\mathbf{k})}\sqrt{1-x^2} \quad , \qquad z(x;\mathbf{k}) = \frac{\hat{\Gamma}(\mathbf{k})}{\alpha}\big(1 + 2x\sqrt{\alpha}\big) \ , \tag{43}$$

where $x \in [-1;1]$. This solution makes sense only for the modes $\mathbf{k}$ and ratios $\alpha$ such that the local semi-circle distributions attached to two contiguous eigenvalues do not overlap. More precisely, the ratio $\alpha$ should be smaller than

$$\alpha_{merging}(\mathbf{k}) \simeq \frac{(\hat{\Gamma}(\mathbf{k}) - \hat{\Gamma}(\mathbf{k}^c))^2}{4(\hat{\Gamma}(\mathbf{k}) + \hat{\Gamma}(\mathbf{k}^c))^2} \ , \tag{44}$$

where $\mathbf{k}^c$ is the momentum vector corresponding to the closest eigenvalue to $\hat{\Gamma}(\mathbf{k})$. This formula gives the values of the ratios at which the small blobs of $\rho(z)$ (Figs. 2(b) and 3) successively merge, and is asymptotically correct for large $|\mathbf{k}|$.

When $\alpha$ is sufficiently large, all blobs have merged into a single continuous, semi-circle distribution, as could be expected from the vanishing correlation between the matrix elements of $\mathbf{C}$, centered in $z_1 = \frac{1}{2}(z_- + z_+) = \hat{\Gamma}_1$ and of half-width $\frac{1}{2}(z_+ - z_-) = 2\sqrt{\hat{\Gamma}_2/\alpha}$, with $\hat{\Gamma}_1 = \sum_{\mathbf{k}\neq\mathbf{0}} \hat{\Gamma}(\mathbf{k})$ and $\hat{\Gamma}_2 = \sum_{\mathbf{k}\neq\mathbf{0}} \hat{\Gamma}(\mathbf{k})^2$.

### C. Eigenvectors of MERM and Fourier modes associated to the ERMs

We briefly discuss here the properties of the eigenvectors of MERM. We consider a blob of eigenvalues originated from the same ERM eigenvalue (labelled by $\mathbf{k}$), see previous section. To quantify how much the MERM eigenvectors $\mathbf{v}$ are related to the $2L$ eigenvectors (Fourier modes) of the $L$ ERMs, we write

$$v_i = \sum_{\ell=1}^{L} \Big(\gamma_\ell \frac{1}{\sqrt{N}} \cos\left(2\pi\, \mathbf{k}\cdot\mathbf{r}_i^\ell\right) + \delta_\ell \frac{1}{\sqrt{N}} \sin\left(2\pi\, \mathbf{k}\cdot\mathbf{r}_i^\ell\right)\Big) + R_i \ , \tag{45}$$

where $\gamma_\ell$ and $\delta_\ell$ are the projection coefficients onto the $2L$ ERMs eigenvectors and $\mathbf{R}$ is the component of $\mathbf{v}$ orthogonal to this subspace.

The distributions of the coefficients $\gamma_\ell, \delta_\ell$ and of the norm of $\mathbf{R}$ are shown in Fig. 4 in the case $L = 5$ and for increasing values of $N$. We observe that

- the magnitude of $\gamma_\ell$ and $\delta_\ell$ seems to be independent of $N$ (Fig. 4(a)), which implies that these coefficients remain finite as $N \to \infty$. Conversely, the projections of $\mathbf{v}$ on Fourier modes attached to a momentum $\mathbf{k}' \neq \mathbf{k}$ vanishes with increasing $N$, see Fig. 4(b). Hence, $\mathbf{v}$ retains some coherence with the $2L$ eigenvectors of the ERMs attached to the blob even in the infinite size limit (provided $L$ remains finite).

- the norm of $\mathbf{R}$ seems to get peaked as $N$ grows around a non-zero value. Therefore, $\mathbf{v}$ has a substantial component outside the $2L$-dimensional subspaces spanned by the ERM eigenmodes.

Notice that the magnitudes of the $\gamma, \delta$ coefficients and of the norm of $\mathbf{R}$ are related to each other through $\langle\gamma^2\rangle = \langle\delta^2\rangle = (1 - \langle\mathbf{R}^2\rangle)/L$ to ensure the normalization of $\mathbf{v}$. The results above were derived for finite $L$ and large $N$; in the double scaling limit where both $L, N$ are large at fixed ratio $\alpha$, we find that the coefficients $\gamma, \delta$ of the projections on the Fourier modes attached to the blob also scale as $N^{-1/2}$, in accordance with the number of those modes.

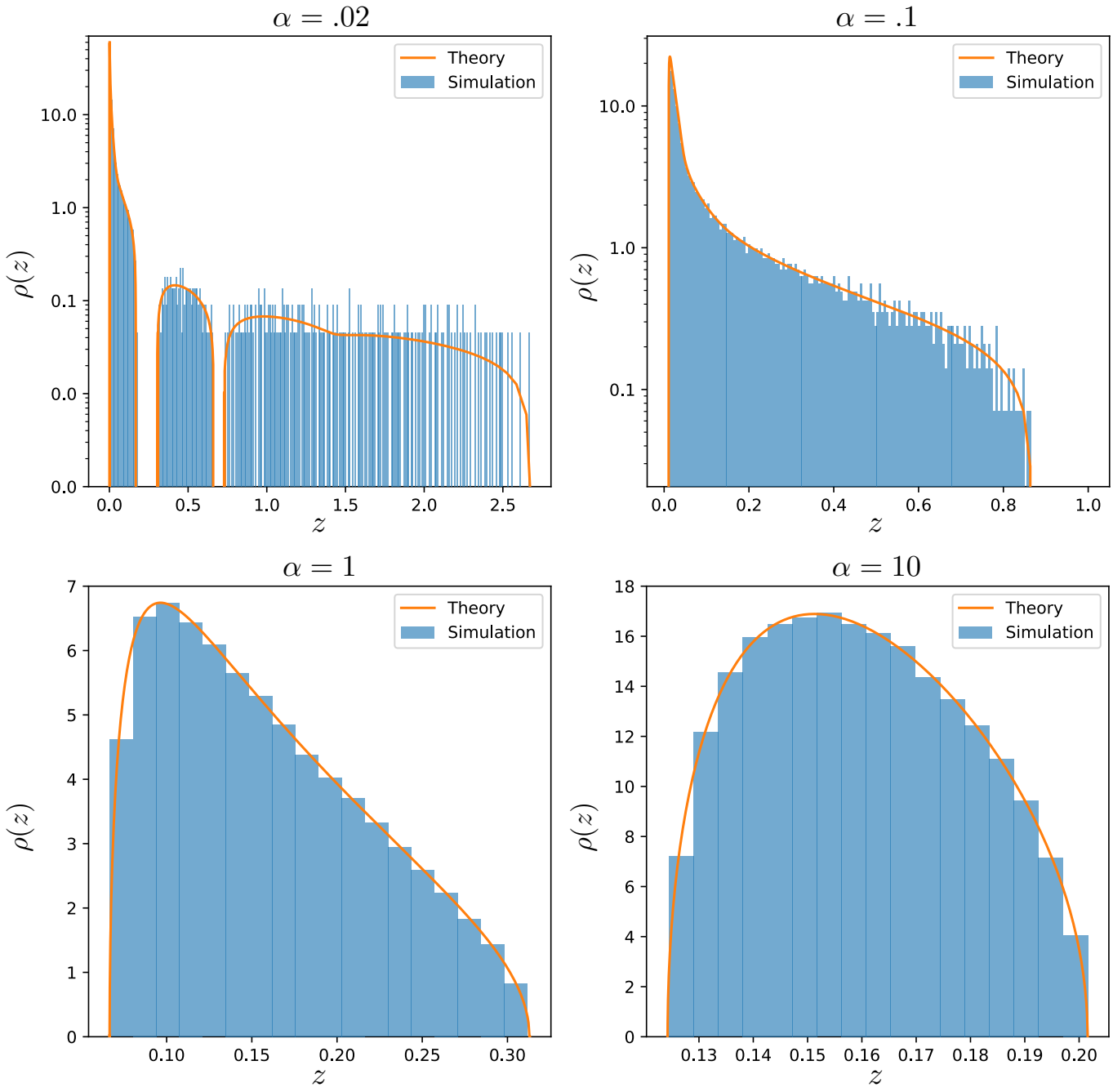


FIG. 3: Density of eigenvalues of $\mathbf{C}$, without the extensive eigenvalue (18), for various values of $\alpha$. Orange: results from (37). Blue: outputs of numerical diagonalization for $N = 2500$. Same model as in Fig. 2.

## V. VARIANTS OF MODEL

The function $\Gamma$ we have considered so far corresponds to the simple model defined in Fig. 1. In a unit cube $\mathcal{H}_D$ in $D$ dimensions, a set of $N$ positions $\mathbf{r}_i^\ell$ (centres of $D$-dimensional spheres of volume $\phi_0 < 1$) are drawn uniformly and independently at random for each "map" $\ell$.

The term $\Gamma\left(\left|\mathbf{r}_i^\ell - \mathbf{r}_j^\ell\right|\right)$ entering in the correlation matrix (2) is simply the overlap (common volume) between the two spheres in the same space, see Fig. 1. We consider below three variants of this model, of interest for computational neuroscience, see Section 6.

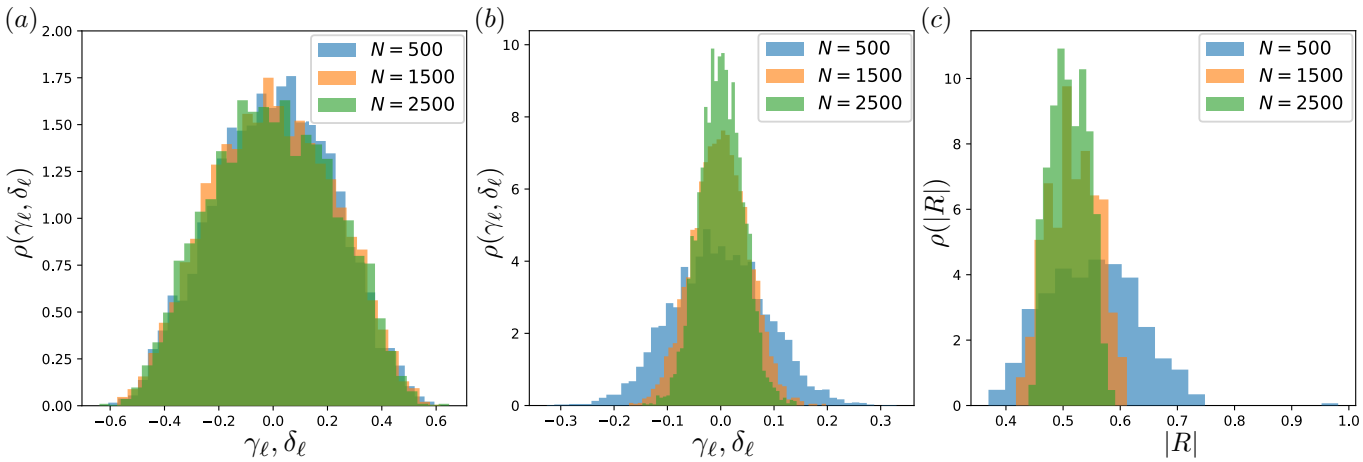


FIG. 4: (a) Histogram of the coefficients $\gamma_\ell$ and $\delta_\ell$ for different values of $N$. Results correspond to the $k = 1$ blob of eigenvalues in dimension $D = 1$ and for $L = 5$ spaces, averaged over 50 samples. Same model as in Fig. 2. (b) Histograms of the projections of eigenvectors $\mathbf{v}$ to the $k = 2$ Fourier modes of the ERMs. (c) Histograms of the norm of the orthogonal component $\mathbf{R}$, see (45).

### A. Dilution

Let us first consider single-space ERM in which a fraction $\rho_0$ of the $N$ positions (chosen at random among $1, ..., N$) carry vanishingly small spheres, and the remaining points are centers of standard spheres of volume $\phi_0$. All the entries of ERM $M_{ij}^{(1)} = \Gamma(|\mathbf{r}_i - \mathbf{r}_j|)/N$ such that $i$ or $j$ belongs to the first subset (with point-like spheres) are equal to zero. We are left with a block matrix of dimension $(1-\rho_0)N \times (1-\rho_0)N$, equal to the ERMs considered so far with the model of Fig. 1. As a consequence, in the large $N$ limit, the eigenvalues of this block-ERM are equal to $\rho_0\, \hat{\Gamma}(\mathbf{k})$, while the remaining eigenvalues are equal to zero.

The resolvent of this diluted version of ERM in the high-density regime has the same form as (6):

$$s_1(z) = -\frac{1}{zN}\left(\rho N + \sum_{\ell=1}^{\infty} \sum_{\mathbf{k}}^{(\rho N)} \hat{\Gamma}(\mathbf{k})^\ell \, \frac{1}{z^\ell} + (1-\rho)N\right) = -\frac{1}{z} - \frac{1}{N\, z}\, \gamma\left(\frac{1}{z}\right) + o\left(\frac{1}{N}\right) \tag{46}$$

where

$$\gamma(u) = \sum_{\mathbf{k}} \frac{u\, \rho_0 \hat{\Gamma}(\mathbf{k})}{1 - u\, \rho_0 \hat{\Gamma}(\mathbf{k})}\,. \tag{47}$$

The computation of the functional inverse of the resolvent of the dilute MERM can be done as in the standard case, and we get:

$$z = \sum_{\mathbf{k}} \frac{\alpha\, \rho_0 \hat{\Gamma}(\mathbf{k})}{\alpha + s\, \rho_0 \hat{\Gamma}(\mathbf{k})} - \frac{1}{s}\,. \tag{48}$$

We can now solve equation (48) in order to get the density of eigenvalues. The agreement with the spectrum obtained from numerical simulations is excellent, see Fig. 5(a).

### B. Spheres of different volumes

We now discuss the case of a multinomial distribution of sphere volumes. We consider first that, in each space, a fraction $\rho_1$ of the $N$ spheres have volume $\phi_1$, while the remaining fraction $\rho_2 = 1 - \rho_1$ have volume $\phi_2$. For every space we build a matrix composed of 4 blocks:

$$\mathbf{M}^{(1)} = \frac{1}{N}\left(\begin{array}{c|c} \mathbf{\Gamma}_{11} & \mathbf{\Gamma}_{12} \\ \hline \mathbf{\Gamma}_{21} & \mathbf{\Gamma}_{22} \end{array}\right)\,, \tag{49}$$

where the block $\mathbf{\Gamma}_{ab}$ is a $\rho_a N \times \rho_b N$ ERM depending on the overlaps between spheres of volumes $\phi_a$ and $\phi_b$, and with $a, b$ taking values 1 or 2. We look for eigenvectors of $\mathbf{M}^{(1)}$ of components $v_i(\mathbf{k}) \propto e^{i\,2\pi\,\mathbf{k}\cdot\mathbf{r}_i}$ multiplied by $\alpha_a$ for the sites $i$ in the fraction $\rho_a$, with $a = 1, 2$. We obtain the following eigen-system :

$$\begin{cases} \rho_1\,\hat{\Gamma}_{11}(\mathbf{k})\;\alpha_1 + \rho_2\,\hat{\Gamma}_{12}(\mathbf{k})\;\alpha_2 = \lambda(\mathbf{k})\;\alpha_1 \\ \rho_1\,\hat{\Gamma}_{21}(\mathbf{k})\;\alpha_1 + \rho_2\,\hat{\Gamma}_{22}(\mathbf{k})\;\alpha_2 = \lambda(\mathbf{k})\;\alpha_2 \end{cases} . \tag{50}$$

In the system above $\hat{\Gamma}_{ab}(\mathbf{k}) = \hat{\gamma}_a(\mathbf{k})\hat{\gamma}_b(\mathbf{k})$ with $a, b$ taking value 1 or 2 and

$$\hat{\gamma}_a(\mathbf{k}) = \int_{\mathcal{H}_D} d\mathbf{r}\,\gamma_a(\mathbf{r})\,e^{i2\pi\mathbf{k}\cdot\mathbf{r}} \tag{51}$$

with $\gamma_a(\mathbf{r})$ being the indicator function of the place field of volume $\phi_a$. We find $\alpha_a \propto \hat{\gamma}_a(\mathbf{k})$ and $\lambda(\mathbf{k}) = \rho_1(\hat{\gamma}_1(\mathbf{k}))^2 + \rho_2(\hat{\gamma}_2(\mathbf{k}))^2$.

This result immediately extends to more than two sphere types. If we have $K$ finite (as $N \to \infty$) types of spheres, with associated volumes $\phi_a$ and fractions $\rho_a$, with $a = 1, ..., K$, the eigenvalue of ERM attached to the momemtum $\mathbf{k}$ is given by

$$\lambda(\mathbf{k}) = \sum_{a=1}^{K} \rho_a\;(\hat{\gamma}(\mathbf{k}))^2\;. \tag{52}$$

It is straightforward to write the resulting self-consistent equation for the MERM resolvent by simply changing $\hat{\Gamma}(\mathbf{k}) \to \sum_{a=1}^{K} \rho_a\;(\hat{\gamma}_{aa}(\mathbf{k}))^2$ in (17). In Fig. 5(b) we show the perfect agreement of this theoretical result with numerical simulations.

### C. Multiple spheres per site in each space

We extend the above setting to the case of multiple spheres per site in each space. More precisely, we assume that for each site $i = 1...N$, there are $n$ centers $\mathbf{r}_{i,m}^{\ell}$ of spheres, with $m = 1, ..., n$ in each space $\ell$; we assume that $n$ remains finite as $N, L$ are sent to infinity. The MERM is defined as follows

$$C_{ij} = \frac{1}{L}\sum_{\ell=1}^{L}\sum_{m,m'=1}^{n} \Gamma\left(\left|\mathbf{r}_{i,m}^{\ell} - \mathbf{r}_{j,m'}^{\ell}\right|\right)\;. \tag{53}$$

To better understand what happens in this case we consider the limit case of a single map:

$$M_{ij}^{(1)} = \frac{1}{N}\sum_{m,m'=1}^{n} \Gamma\left(\left|\mathbf{r}_{i,m} - \mathbf{r}_{j,m'}\right|\right)\;. \tag{54}$$

In the high-density regime the eigenvectors of this ERM have components $v_i(\mathbf{k}) \propto \sum_m e^{i\,2\pi\,\mathbf{k}\cdot\mathbf{r}_{i,m}}$ with eigenvalues equal to $n\,\hat{\Gamma}(\mathbf{k})$ (for $\mathbf{k} \neq \mathbf{0}$). The only change to the functional inverse of the MERM resolvent is $\hat{\Gamma}(\mathbf{k}) \to n\;\hat{\Gamma}(\mathbf{k})$, so that we obtain:

$$z = \sum_{\mathbf{k}} \frac{\alpha\,n\,\hat{\Gamma}(\mathbf{k})}{\alpha + s\,n\,\hat{\Gamma}(\mathbf{k})} - \frac{1}{s}\,. \tag{55}$$

We have solved equation (55) in order to get the density of eigenvalues; results are in excellent agreement with numerics, see Fig. 5(c).

## VI. CONCLUSION

In this work we have introduced a novel statistical ensemble for Euclidean random matrices (ERM), where the element $i, j$ of the matrix depend on the distances between representative points of $i$ and $j$ in more than one space. We have shown that the high-density limit is non trivial when the number $L$ of spaces and the size $N$ of the matrix

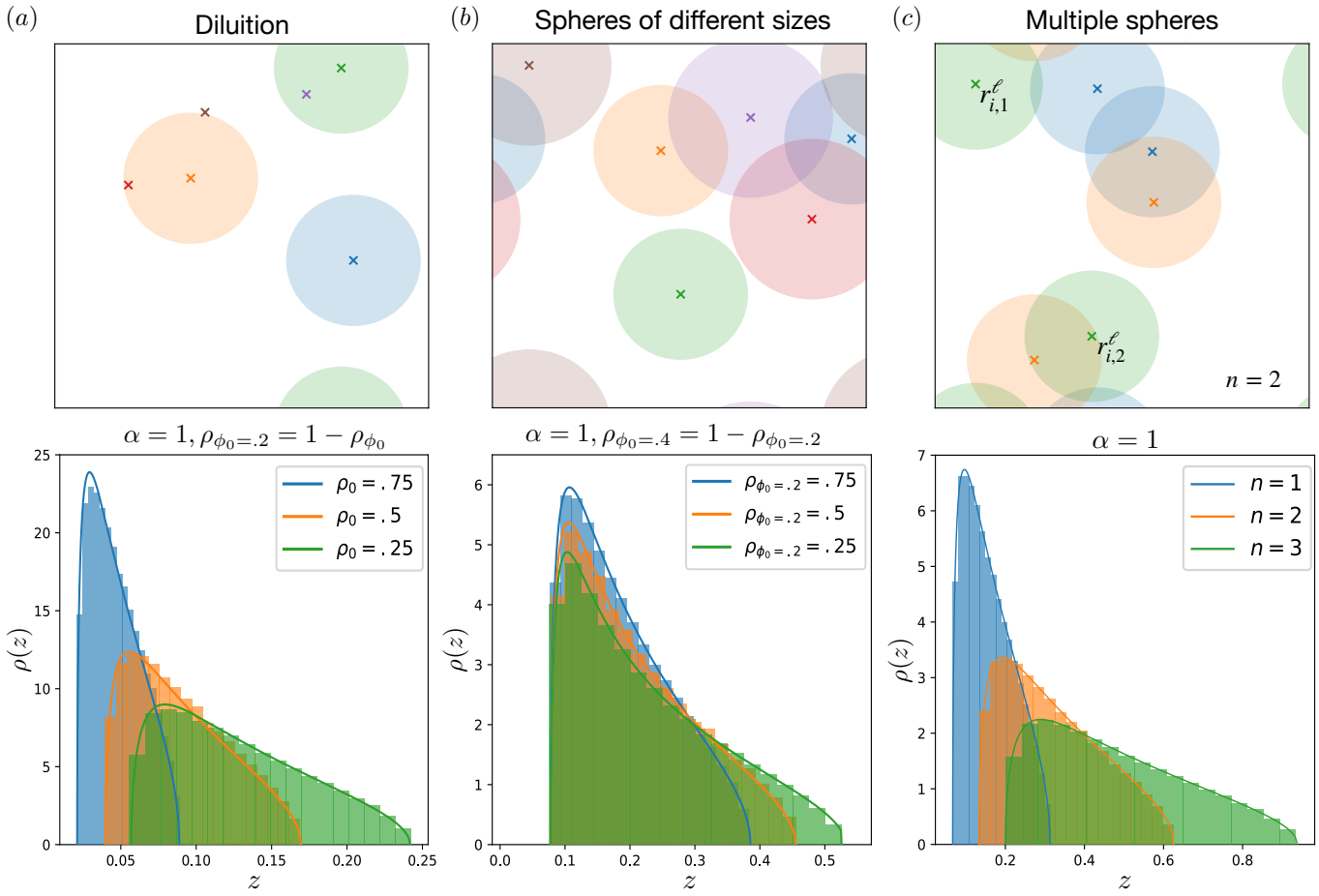


FIG. 5: Top panels: sketches of the model variants, respectively $(a)$ dilution, $(b)$ spheres of different sizes and $(c)$ multiple spheres. Bottom panels: $(a)$ Density of eigenvalues for the MERM for $\phi_0 = .2$ with different dilution fractions $\rho_0$. $(b)$ Density of eigenvalues of MERM with different fractions $\rho_{\phi_0=.2}$ of spheres with volume $\phi_0 = .2$ and $\rho_{\phi_0=.4}$ of spheres with volume $\phi_0 = .4$ in each space. $(c)$ Density of eigenvalues of MERM for $\phi_0 = .2$ with $n$ spheres for each index $i$ in each map. Parameters: $N = 2500, D = 1, \alpha = 1$. In all cases we do not show the extensive eigenvalue.

are sent to infinity, with a fixed ratio $\alpha = L/N$. We have analytically studied the density of eigenvalues of this Multiple-space–ERM (MERM) ensemble, based on free-probability identities and on the replica method. Our results are in very good agreement with numerical simulations for all the cases we have considered.

Our motivation to introduce and study MERM came from computational neuroscience [11], in particular the modeling of spatial representations in the mammalian hippocampus. The activity of place cells strongly depends on the position of the animal in the environment, defining spatial place fields in which they are active. Experiments on rodents and bats show that place fields are approximately disks in two-dimensional environments and spheres in three dimensions. Our basic model, shown in Fig. 1, assumes that all place fields cover the same area/volume. However, in the CA3 region of the hippocampus in particular, neurons may have place fields in some environment and none in other environments, which corresponds to the dilute model introduced in Section 5. In addition, we have introduced other variants, in which the radius of place fields varies or a place field is made of more than one connected spatial component, as seen in large environments [15]. While the variants of the model considered here lead to different densities of eigenvalues $z$, the behaviours of these densities for $z \to 0$ and $\alpha \to 0$ seem qualitatively robust, which suggests that the storage capacity of recurrent neural networks is a robust property of the space-to-neural activity encoding [11].

In addition to the neuroscience motivation reported above, we hope that MERM will find applications and be of interest in other fields, e.g. in applied mathematics or in information theory. In particular, our results could be used for functions $\Gamma$ with a dependence on the pairwise distances different from the ones considered in this article. From a random matrix point of view, it would also be natural to consider models for MERM, where the statistical features of the $L$ ERM's are non independent from space to space. In the context of place cells and fields, it is known

that neurons have some individuality, that is, retain some properties in the different environments. In particular it was reported experimentally [15, 16] that each place cell has its own propensity to have one place field per square meter: many neurons have very low propensity values, *i.e.*, have no place field at all in many maps as in Fig. 5(a), and few neurons that have very high propensity and therefore tend to code almost all maps even with more than one place field connected component per map (Fig. 5(c)). It would be very interesting to study the consequences of non-independence between the elementary ERM's composing the MERM on the density of eigenvalues and the structure of the eigenvectors.

**Acknowledgements.** We are grateful to Yue M. Lu for interesting discussions. This work was funded by the HFSP RGP0057/2016 project.

[1] M. Mézard, G. Parisi and A. Zee. "Spectra of Euclidean random matrices." Nuclear Physics B 559.3: 689-701, (1999).
[2] G. Parisi. "Euclidean random matrices, the glass transition and the boson peak". The European Physical Journal E, 9(3), 213-218, (2002).
[3] T. S. Grigera, V. Martin-Mayor, G. Parisi and P. Verrocchio. "Vibrations in glasses and Euclidean random matrix theory". Journal of Physics: Condensed Matter, 14(9), 2167, (2002).
[4] T. S. Grigera, V. Martin-Mayor, G. Parisi, P. Urbani and P. Verrocchio. "On the high-density expansion for Euclidean random matrices". Journal of Statistical Mechanics: Theory and Experiment, 2011(02), P02015, (2011).
[5] S. E. Skipetrov and A. Goetschy. "Eigenvalue distributions of large Euclidean random matrices for waves in random media". arXiv preprint arXiv:1007.1379, (2010).
[6] A. Goetschy and S. E. Skipetrov. "Non-Hermitian Euclidean random matrix theory". Physical Review E, 84(1), 011150, (2011).
[7] S. Ciliberti, T. S. Grigera, V. Martn-Mayor, G. Parisi and P. Verrocchio. "Anderson localization in Euclidean random matrices". Physical Review B, 71(15), 153104, (2005).
[8] A. Amir, Y. Oreg and Y. Imry. "Localization, anomalous diffusion, and slow relaxations: A random distance matrix approach". Physical review letters, 105(7), 070601, (2010).
[9] A. Goetschy and S. E. Skipetrov. "Euclidean random matrices and their applications in physics". arXiv preprint arXiv:1303.2880, (2013).
[10] C. Bordenave. "Eigenvalues of Euclidean random matrices". Random Structures and Algorithms, 33(4), 515-532, (2008).
[11] A. Battista and R. Monasson. "Capacity-Resolution Trade-Off in the Optimal Learning of Multiple Low-Dimensional Manifolds by Attractor Neural Networks". Physical Review Letters, 124(4), 048302, (2020).
[12] G. Livan, M. Novaes and P. Vivo. "Introduction to random matrices: theory and practice". Springer International Publishing, (2018).
[13] J. A. Mingo and R. Speicher. "Free probability and random matrices" (Vol. 35). New York: Springer, (2017).
[14] M. Mézard, G. Parisi and M. Virasoro. "Spin glass theory and beyond: An Introduction to the Replica Method and Its Applications". Vol. 9. World Scientific Publishing Company, (1987).
[15] P. D. Rich , H. P. Liaw and A. K. Lee. "Large environments reveal the statistical structure governing hippocampal representations". Science, 345(6198), 814-817, (2014).
[16] J. S. Lee, J. Briguglio, S. Romani and A. K. Lee. "The statistical structure of the hippocampal code for space as a function of time, context, and value". bioRxiv, 615203, (2019).